Magnesium Technology 2011
Edited by: Wim H. Sillekens, Sean R. Agnew, Neale R. Neelameggham, and Suveen N. Mathaudhu
TMS (The Minerals, Metals & Materials Society), 2011

APPLICABILITY OF Mg -Zn-(Y, Gd) ALLOYS FOR ENGINE PISTONS

Kazutaka Okamoto[1], Masato Sasaki[2], Norikazu Takahashi[2], Qudong Wang[3], Yan Gao[3], Dongdi Yin[3], Changjiang Chen[3]
[1]Hitachi, Ltd.; Hitachi, Ibaraki 319-1292, Japan
[2]Hitachi Automotive Systems, Ltd.; Atsugi, Kanagawa 243-8510, Japan
[3]Shanghai Jiao Tong Univ.; Shanghai 200240, China

Keywords: Gravity casting, Heat treatment, Tensile strength, Creep strain, Fatigue strength

Abstract

Commercial magnesium alloys have a great potential for structural applications in automotive due to their significant weight saving. However, they have poor creep resistance at temperature over 125°C, thus making them inadequate for power train applications such as engine pistons, which are operated at temperature up to 300°C. Recently, creep resistant magnesium alloys with rare-earth elements and Zn have been developed, hence the applicability of Mg-Zn-(Y, Gd) alloys for engine pistons was investigated in this paper. Gravity casting was performed with Mg-Zn-(Y, Gd)-Zr alloy, followed by T6 treatment. Effects of the amount of alloying elements on the mechanical properties of tensile strength and creep strain were evaluated. Nominal composition of Mg-2Zn-11Y-5Gd-0.5Zr was selected for the actual piston cast trial and its high cycle fatigue test was conducted comparing to the current aluminum cast alloy of A336 (JIS AC8A) for pistons. At room temperature, the fatigue strength is 27% lower than A336, while it is 35% higher at 300°C. It is suggested that Mg-2Zn-11Y-5Gd-0.5Zr alloy shows attractive high temperature mechanical properties higher than A336, hence it is promising as a candidate material for the engine piston application.

Introduction

Magnesium alloys have a great potential for structural applications in automotive and aerospace industries due to their significant weight savings, thus improving fuel economy and lessening environmental impact. The most significant magnesium applications are in castings, such as instrument panel, transfer cases, valve/cam covers, various housings and brackets, and steering components in automobiles, with commercial magnesium alloys of AZ91, AM50 and AM60. These alloys offer an excellent combination of mechanical properties, corrosion resistance and castability.

On the other hand, power train components are made of heavy parts, hence the specific weight of magnesium, which is 2/3 of aluminum, is very attractive for weight reduction of transmission case or engine block. Although aluminum engine piston is not so weighty, generally about 0.3kg, it is reciprocated at higher velocity over 10m/s, so that the reciprocating mass can be reduced. Furthermore, weight reduction of circumference parts such as connecting rod, less NVH (Noise, Vibration and Harshness) issues, higher performance of engine are expected. However, these components are operated at higher temperatures above 175°C, engine block up to 200°C, and engine pistons up to 300°C, thus making commercial magnesium alloys inadequate for major power-train applications because of their poor creep resistance at temperatures above 125°C.

The requirements for high temperature creep resistance and weight savings have made it imperative to develop new magnesium alloys to decrease use of conventional aluminum and iron castings in vehicles. Both diffusion controlled dislocation climb and grain boundary sliding/shearing have been reported as creep mechanisms in magnesium alloys, depending on the alloy system, microstructure, and stress and temperature regimes. In magnesium alloys, aluminum is often added to obtain a good combination of strength, ductility and castabilty. However, the poor thermal stability of $Mg_{17}Al_{12}$ intermetallics (β phase, with a eutectic temperature of 437°C) and its discontinuous precipitation can result in substantial grain boundary sliding/shearing at elevated temperatures. Moreover, the accelerated diffusion of aluminum solute in magnesium matrix and the self-diffusion of magnesium at elevated temperatures contribute to creep deformation in Mg-Al based alloys. Based on the above arguments and alloy strengthening mechanisms, possible approaches to improve creep resistance in magnesium alloys include solution strengthening, precipitation strengthening and dispersoid strengthening. Most of magnesium alloy systems were developed using these approaches to obtain good elevated/high-temperature creep resistance, namely Mg-Al-Sr (AJ), Mg-Al-Ca(-Sr) (AX(J)), Mg-Al-RE (AE), Mg-Y-Nd (WE), etc. Among those alloys, the enhancement of creep resistance by rare earth (RE) elements is particularly common. RE has a quite large solubility, resulting in solid solution strengthening, decreasing stacking fault energy, thus splitting basal dislocation into partials and increasing resistance of dislocation glide and climb [1-3]. Furthermore, Zn addition significantly enhances the age hardening response and the creep resistance with uniform and dense distribution of basal precipitate plates [4] and/or long period stacking order (LPSO) [5-13], namely Mg-Zn-RE alloy.

In this research, high temperature properties of Mg-Zn-(Y, Gd) cast alloy were evaluated so as to investigate the applicability of the cast to engine pistons, considering those of the current aluminum cast alloy of A336 (JIS AC8A). Conventional gravity casting was carried out, followed by T6 heat treatment, and both creep strain and high cycle fatigue tests as well as tensile test at room and elevated temperature were conducted. Our development goal was set as summarized in Table 1.

Table 1 Development goal for the mechanical properties of Mg-Zn-(Y, Gd) cast alloy

Property and Test Conditions	Goal
Ultimate Tensile Strength	
RT	> 230MPa
300°C	> 150MPa
Creep Strain	
250°C , 80MPa for 20hrs	< 0.30%
300°C , 50MPa for 20hrs	< 0.40%
Fatigue Strength	
300°C, 10^7cycles	> 65MPa

Experimental

Materials to be Evaluated

The chemical compositions of the magnesium alloys are summarized in Table 2. The actual chemical composition of the alloys were evaluated by an inductively couples plasma (ICP).

All these alloy master ingots were prepared with high purity Mg (99.95%) and Zn (99.95%), Mg-25mass%Gd, Mg-25mass%Y and Mg-30mass%Zr alloys. After smelting using an electric resistance furnace under the mixed cover gas of CO_2 and SF_6, the molten metal was pored into a preheated (200°C) cast iron block mold with a wall thickness of 20mm, see Fig.1.

Table 2 Nominal and actual chemical composition of Mg-Zn-(Y, Gd)-Zr cast alloy (mass %)

Nominal comp.	Actual comp.				
	Zn	Y	Gd	Zr	Mg
Mg-10Y-5Gd-0.5Zr	-	8.9	5.4	0.4	bal.
Mg-2Zn-**10Y-5Gd**-0.5Zr	2.1	10.5	4.6	0.4	bal.
Mg-2Zn-**5Y-15Gd**-0.5Zr	1.9	3.6	12.5	0.4	bal.
Mg-2Zn-**5Y-5Gd**-0.5Zr	2.3	4.1	5.0	0.4	bal.
Mg-2Zn-**11Y**-5Gd-0.5Zr	2.2	10.7	5.6	0.4	bal.
Mg-2Zn-**12Y**-5Gd-0.5Zr	2.0	11.9	5.6	0.4	bal.
Mg-2Zn-**14Y**-5Gd-0.5Zr	2.2	14.4	4.9	0.5	bal.
Mg-**0.5Zn**-10Y-5Gd-0.5Zr	0.6	7.2	4.1	0.4	bal.
Mg-**2Zn**-10Y-5Gd-0.5Zr	2.1	10.5	4.6	0.4	bal.
Mg-**3Zn**-10Y-5Gd-0.5Zr	3.5	9.1	4.8	0.5	bal

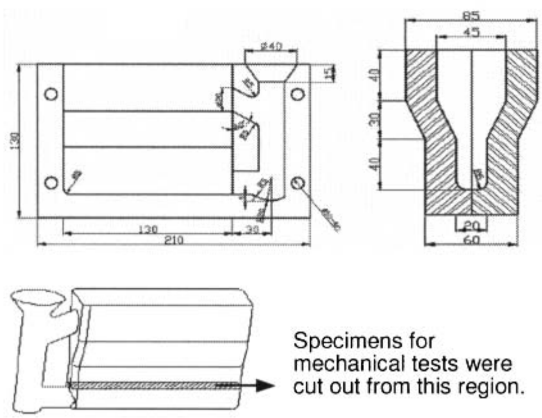

Fig. 1 Schematic drawings of cast iron block mold

Microstructure and Hardness

Microstructure observation was carried out using an optical microscope (OM) and a scanning electron microscope equipped with an energy dispersive X-ray spectrometer (SEM-EDS). Specimens were cut and polished, then etched with 5mass% HNO_3 ethanol. Differential scanning calorimetry (DSC) as well as Vickers hardness tests with an indentation load of 49N were also performed in order to decide the heat treatment condition.

Mechanical Properties

Mechanical properties were evaluated with the specimens shown in Fig. 2, cut from the cast magnesium alloy. Tensile test was performed at both room and elevated temperatures with an initial strain rate of 0.5mm/min. Creep strain was evaluated at 200°C, 250°C and 300°C with an initial load of 120MPa, 80MPa and 50MPa, respectively. Furthermore, high cycle tensile-tensile fatigue test was carried out at room temperature, 250°C and 300°C, up to 10^7 cycles. The stress ratio and frequency were set to R=0 and 30Hz, respectively.

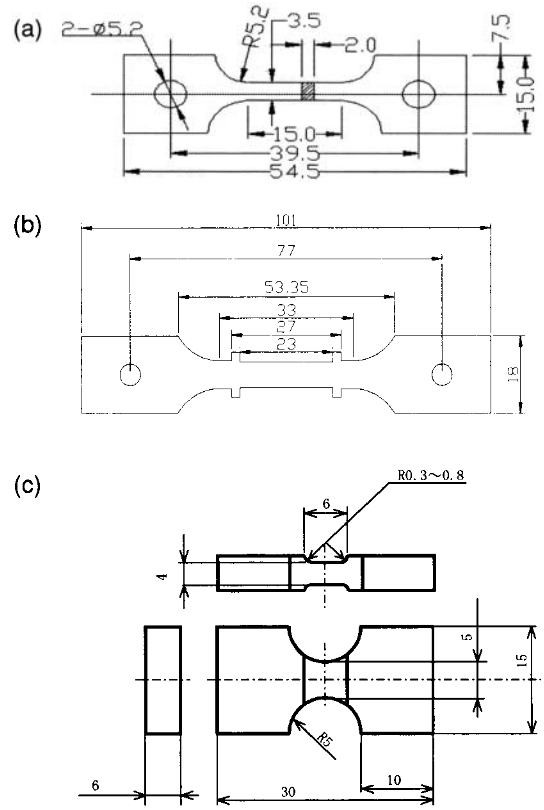

Fig. 2 Schematic drawings of mechanical test specimens for (a) tensile test, (b) creep test and (c) fatigue test

Results and Discussions

Heat Treatment

DSC was conducted for both Mg-10Y-5Gd-0.5Zr and Mg-2Zn-10Y-5Gd-0.5Zr alloys as shown in Fig. 3, and the peak temperatures were measured at 567°C and 540°C, respectively. In order to apply a same heat treatment condition to both alloys, temperature for solution heat treatment was set to 535°C, just below the eutectic temperature of Mg-2Zn-10Y-5Gd-0.5Zr alloy.

Figure 4 shows as-cast and as-T4 microstructure of both alloys. According to the previous research [14], by adding Zn, the resultant microstructure is remarkably changed with long period stacking order formation (seen as a lamellar like morphology in Fig. 4). After 16hrs at 535°C, the eutectic intermetallics of Mg-(Y, Gd) were almost solutionized in α–Mg matrix of Mg-10Y-5Gd-0.5Zr alloy, while the remnant of the eutectic intermetallics was still observed in Mg-2Zn-10Y-5Gd-0.5Zr alloy so that Zn addition decreases the solubility of Y and Gd into α-Mg matrix. The average grain size was approximately 100μm.

After the solution heat treatment, aging treatment was applied at various temperature of 225, 250 and 300°C. Figure 5 shows the age hardening response of Mg-10Y-5Gd-0.5Zr alloy. The peak hardness decreased with increasing aging temperature. At 225°C, the hardness increased rapidly by holding 1hr, and the peak hardness of around135Hv was obtained at about 16-24hrs. After reaching the peak hardness, a plateau region was observed up to 64hrs, then the hardness gradually decreased.

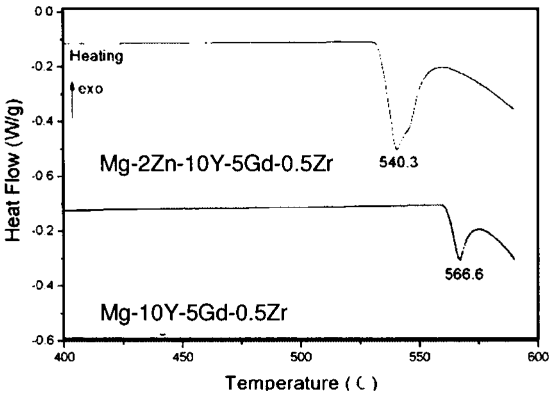

Fig.3 DCS curves for the magnesium alloys

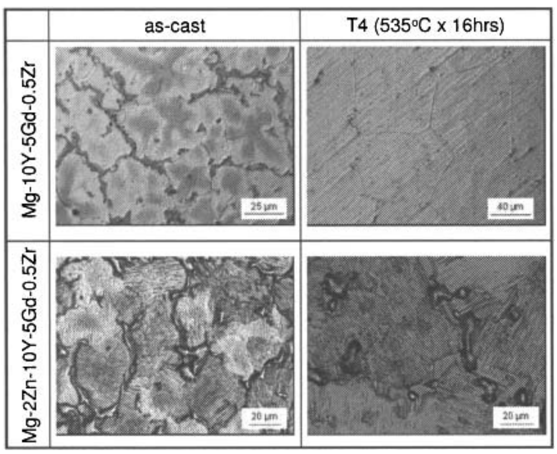

Fig.4 Microstructure of the magnesium alloys

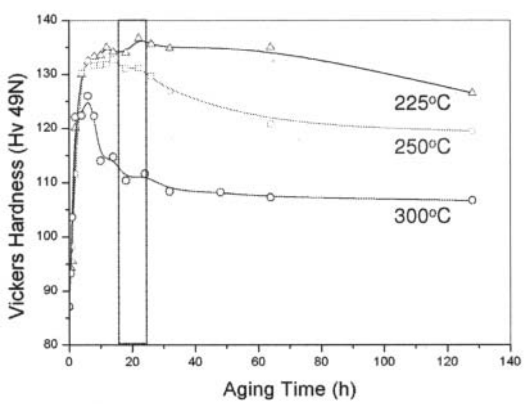

Fig.5 Age hardening response of Mg-10Y-5Gd-0.5Zr alloy

Tensile Strength

In order to investigate the effects of the total amount of RE elements, effects of Y and Gd content on the tensile properties were evaluated. Table 3 summarizes the tensile properties of Mg-2Zn-(Y, Gd)-0.5Zr alloys. It is clearly shown that both 0.2% proof stress ($\sigma_{0.2}$) and ultimate tensile strength (UTS) increased with increasing the total amount of (Y, Gd) while the elongation (ε) remarkably decreased down to less than 1%. However, the melt loss is quite significant for Mg-2Zn-5Y-15Gd-0.5Zr alloy, so that the amount of Gd was selected to 5mass %. Figure 6 shows stress-strain curves of Mg-2Zn-10Y-5Gd-0.5Zr alloy at 300°C and 350°C, respectively. Even at 300°C, UTS is higher than 200MPa, which meets our development goal. However, UTS remarkably decreased over 300°C with significant increase in the elongation up to 28%.

Table 3 Effect of (Y, Gd) on the tensile properties

	$\sigma_{0.2}$ / MPa	UTS / MPa	ε (%)
Mg-2Zn-**10Y-5Gd**-0.5Zr	248	273	0.6
Mg-2Zn-**5Y-15Gd**-0.5Zr	236	305	0.9
Mg-2Zn-**5Y-5Gd**-0.5Zr	126	251	12

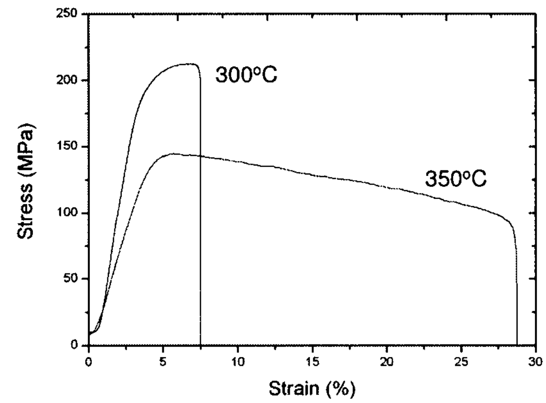

Fig. 6 Stress-strain curves of Mg-2Zn-10Y-5Gd-0.5Zr alloy at elevated temperatures

Creep Strain

In order to determine the composition range, effects of Zn and Y content on the creep properties were investigated.

It was found that the addition of Zn to Mg-10Y-5Gd-0.5Zr alloy remarkably improves the creep resistance, as shown in Table 4, summarizing the creep strain and secondary creep rate at 250°C, 80MPa. Furthermore, Zn content of 2mass % is most affective for the improvement of creep resistance.

Figure 7 shows creep curves of the magnesium alloys at 300°C, 50MPa. Amount of Y, a primary alloying element for these magnesium alloys, has a strong influence on the creep strain. Creep stain is minimized and our goal was achieved for the alloys with Y content of 11-12mass %. However higher Y was demonstrated to be not beneficial for the improvement of creep resistance and the material cost will increase. According to Mg-Y binary diagram, the maximum solubility of Y into α-Mg matrix at the eutectic temperature is about 12.5mass %, hence over high Y addition results in the existence of large amount of eutectic phase, which can not be dissolved into the matrix completely even after the solution heat treatment. These thermal unstable intemetallic compounds may deteriorate the creep resistance at α-Mg grain boundaries.

Figure 8 shows the microstructure evolution of Mg-2Zn-11Y-5Gd-0.5Zr alloy during the creep test at 300°C, 50MPa for 0-100hrs. It can be seen that the lamellar like morphology is developed as increasing the testing time and maybe the structure causes higher creep resistance.

Table 4 Effect of Zn on the creep properties at 250°C, 80MPa

	Creep strain for 20hrs (%)	Secondary creep rate / s^{-1}
Mg-10Y-5Gd-0.5Zr	0.36	44.6×10^{-9}
Mg-**0.5Zn**-10Y-5Gd-0.5Zr	0.16	6.19×10^{-9}
Mg-**2Zn**-10Y-5Gd-0.5Zr	0.12	3.89×10^{-9}
Mg-**3Zn**-10Y-5Gd-0.5Zr	0.28	11.8×10^{-9}

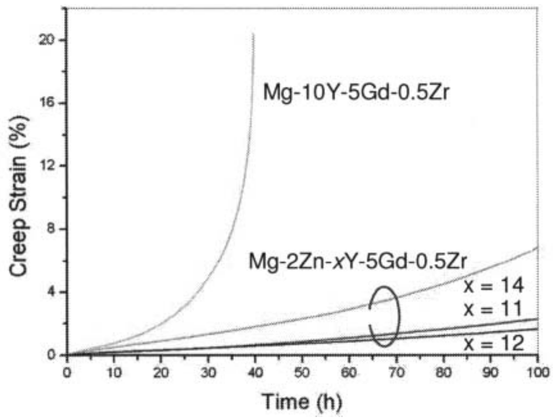

Fig. 7 Creep curves of the magnesium alloys at 300°C, 50MPa

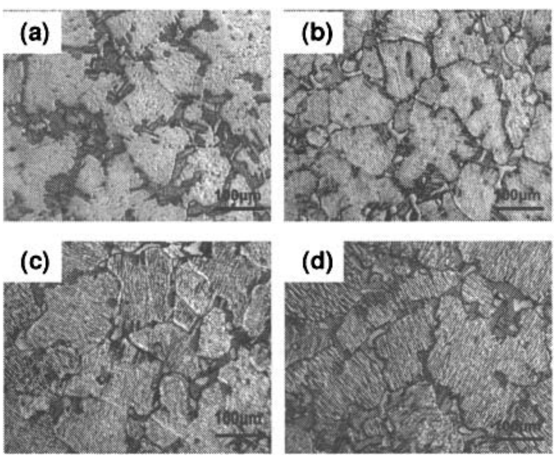

Fig.8 Microstructure evolution in Mg-2Zn-11Y-5Gd-0.5Zr alloy during the creep test at 300°C for (a) 0hr, (b) 20hrs, (c) 50hrs and (d) 100hrs

Fatigue Strength

Based on the mechanical properties of various Mg-Zn-(Y, Gd)-Zr alloys above mentioned, Mg-2Zn-11Y-5Gd-0.5Zr alloy was selected for further investigations. Table 5 summarizes the high cycle tensile-tensile fatigue test at room temperature, 250°C and 300°C, comparing to those of A336-T6. Although the fatigue strength of the magnesium alloy at room temperature and 250°C is 30-40% lower than A336, it is about 85% of A336 at 300°C.

Microstructure evolution was observed after the tests at 250°C and 300°C, within the α-Mg grain interior near the boundaries as described in Fig. 9, which may strengthen the grain boundaries and prevent its deformation.

Figure 10 shows the fracture surface of Mg-2Zn-11Y-5Gd-0.5Zr alloy. It is observed that cleavage like cracks are predominant and facet size of the cleavage plane is almost the same as the grain size. Furthermore, fatigue crack propagates perpendicular to the small steps, so that it is considered that the LPSO along with the basal plane of hexagonal α-Mg results in the cleavage cracks.

Table 5 High cycle fatigue strength of Mg-2Zn-11Y-5Gd-0.5Zr and A336 aluminum alloys

	RT	250°C	300°C
Mg-2Zn-11Y-5Gd-0.5Zr	70MPa	59MPa	53MPa
A336	103MPa	96MPa	63MPa

Fig. 9 Microstructure of Mg-2Zn-11Y-5Gd-0.5Zr alloy after testing for 9.5×10^{6} cycles at 55MPa, 300°C

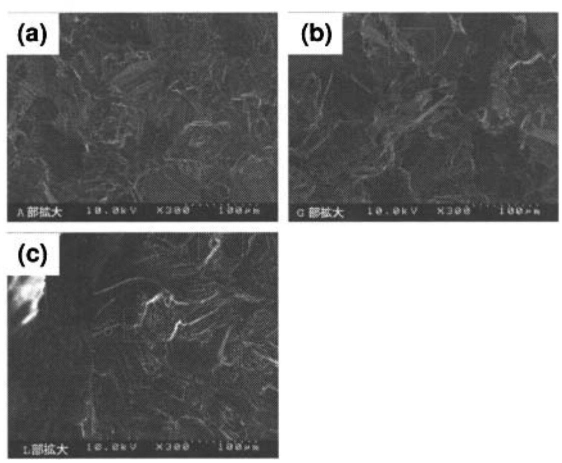

Fig. 10 Fracture surface of fatigue specimens of Mg-2Zn-11Y-5Gd-0.5Zr alloy tested at (a) RT, (b) 250°C and (c) 300°C

Piston Cast Trial

Gravity casting was performed using a piston mold illustrated in Fig. 11. Specimens were cut out from the crown surface for metallurgical and mechanical investigations. The actual chemical composition is analyzed to Mg-2.1Zn-10.9Y-4.6Gd-0.4Zr (mass %). T6 of 535°Cx16-20hrs and 225°Cx24hrs was applied.

Figure 12 show both as-cast and as-T6 microstructures. In case of as-cast, Gd is enriched in α-Mg matrix, whose average grain size is about 100μm, while it is grown to about 150μm via T6 treatment. Zn and Y are detected in the eutectic intermetallics at α-Mg grain boundaries. Furthermore, lamellar like morphology is observed along the α-Mg grain boundaries, which suggests LPSO is formed originated from Y element [6-9]. Yamasaki et al. [9] reported that RE can be categorized into two types; type-I additives such as Y form LPSO during solidification, and type-II additives such as Gd form during high temperature exposure. In case of as-T6, it is suggested that Gd plays an important role forming LPSO. Furthermore, Yamada [11, 12] and Honma [13] reported that 0.3-1.0at. % Zn containing Mg-Gd-Y-Zr alloy shows room temperature tensile strength over 400MPa with 14H-LPSO at α-Mg grain boundaries and metastable β' phase, via solution heat treatment at 500°C followed by aging treatment at 225°C. Therefore, it is considered that the similar type of microstructure evolution can be expected for this alloy.

Figure 13 shows the tensile properties of Mg-2Zn-11Y-5Gd-0.5Zr alloy. It is observed that UTS shows an inverse temperature dependence up to 200°C, and it decreases over the temperature. As mentioned above, the aging treatment at 225°C might form metastable β' phase, so that further investigations of microstructure evolution and phase stability of the resultant microstructure are required. Table 6 summarized the creep properties of Mg-2Zn-11Y-5Gd-0.5Zr alloy at elevated temperatures. It can be said that the creep resistance of the piston specimen is almost comparable to that of block specimen.

Table 6 Creep properties of Mg-2Zn-11Y-5Gd-0.5Zr alloy at elevated temperatures

Temperature / °C	Creep strain for 20hrs (%)	Secondary creep rate / s^{-1}
200	0.17	0.97×10^{-9}
250	0.32	3.65×10^{-9}
300	0.33	4.72×10^{-9}

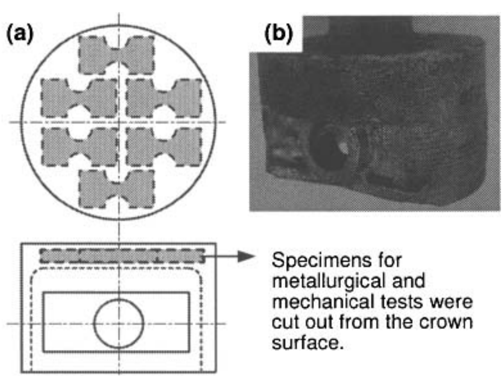

Fig.11 Actual piston cast trial
(a) schematic drawing of piston, (b) as-cast piston

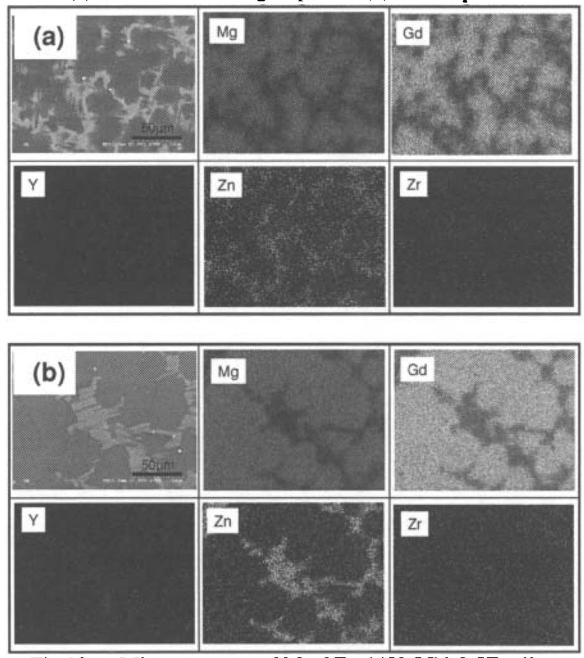

Fig.12 Microstructure of Mg-2Zn-11Y-5Gd-0.5Zr alloy
(a) as-cast and (b) as-T6

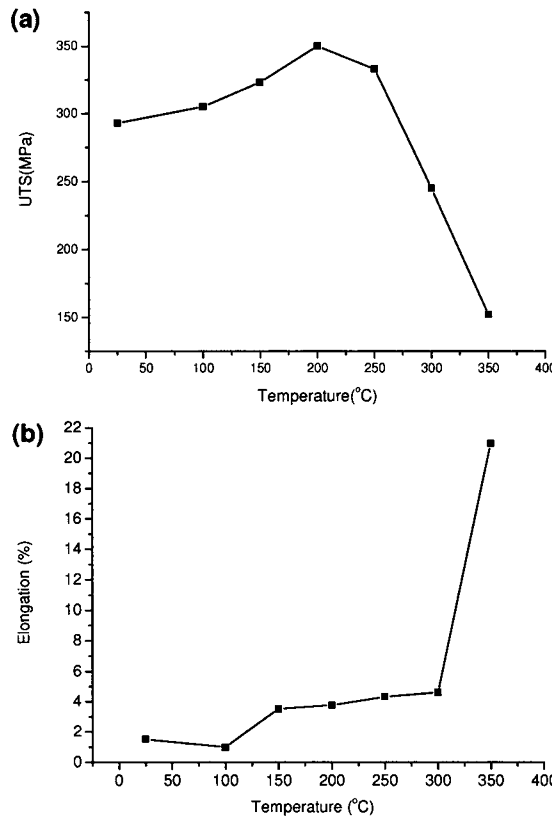

Fig.13 Tensile properties of Mg-2Zn-11Y-5Gd-0.5Zr alloy
(a) UTS and (b) elongation

Table 7 summarizes the high cycle tensile-tensile fatigue test at room temperature, 250°C and 300°C, comparing to those of A336-T6. Similar to the results of the block samples described in Table 5, the fatigue strength at room temperature is 27% lower than A336, while almost the same or even 35% higher strength were obtained at 250°C or 300°C. It is thought that the average grain size of piston crown surface is 150µm, larger than that of the block sample, so that the cooling rate may significantly affect the LPSO formation. Furthermore, microstructure evolution was also observed during the tests at 250°C and 300°C as seen in Fig. 14.

Table 7 High cycle fatigue strength of Mg-2Zn-11Y-5Gd-0.5Zr and A336 aluminum alloys

	RT	250°C	300°C
Mg-2Zn-11Y-5Gd-0.5Zr	75MPa	90MPa	85MPa
A336	103MPa	96MPa	63MPa

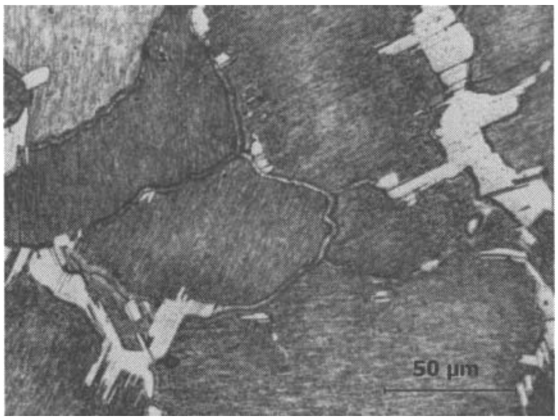

Fig. 14 Microstructure of Mg-2Zn-11Y-5Gd-0.5Zr alloy after testing for 3.3×10^6 cycles at 90MPa, 300°C

Conclusions

Mechanical properties of Mg-Zn-(Y, Gd) alloys were evaluated by using gravity cast and T6 treated specimens and its applicability for engine pistons was investigated. The results obtained are summarized as follows:

- Effect of the amount of the alloying elements, Zn and Y of Mg-*x*Zn-*y*Y-5Gd-0.5Zr (mass %) alloy on the creep property at elevated temperature were studied. It is suggested that the addition of 2mass %Zn and 11mass %Y minimizes the creep stain at elevated temperatures.
- Mg-2Zn-11Y-5Gd-0.5Zr alloy was selected for high cycle fatigue test. Fatigue strength at room temperature and 250°C is 30-40% lower than A336, while it is about 85% of A336 at 300°C.
- Actual pistons of Mg-2.1Zn-10.9Y-4.6Gd-0.4Zr (mass %) were gravity cast. In the comparison to A336, almost the same or even 35% higher fatigue strength were obtained at 250°C or 300°C.

Mg-2Zn-11Y-5Gd-0.5Zr cast alloy exhibits excellent high temperature mechanical properties such as tensile strength, creep resistance and fatigue strength, equivalent or even higher in the comparison with the current aluminum alloy for piston. Therefore, it can be concluded that this magnesium alloy is very promising as a candidate material for piston applications, since specific strength design for this alloy piston is not required. However, there are still manufacturing related issues remained, such as optimization of casting design, heat treatment schedule for the stability of microstructure at elevated temperatures, wear resistant surface treatment strategy, and so on. Therefore further investigations are on going via piston trial manufacturing to pursue technical possibility of Mg-Zn-(Y, Gd) alloys for engine pistons.

References

1. I.A.Anyanwu, S.Kamado and Y.Kojima: "Aging characteristics and high temperature tensile properties of Mg-Gd-Y-Zr alloys", Mater. Trans. 42 (2001), pp. 1206-1211
2. I.A.Anyanwu, S.Kamado and Y.Kojima: "Creep properties of Mg-Gd-Y-Zr alloys", Mater. Trans. 42 (2001), pp. 1212-1218
3. Y.Gao, Q.Wang, J.Gu, Y.Zhao, Y.Tong and J.Kaneda: "Effects of heat treatments on microstructure and mechanical properties of Mg-15Gd-5Y-0.5Zr alloy", J. of Rare Earth 26 (2008), pp. 298-302
4. J.F.Nie, X. Gao and S.M. Zhu: "Enhanced age hardening response and creep resistance of Mg-Gd alloys containing Zn", Scripta Mater. 53 (2005), pp. 1049–1053
5. Y.Kawamura, K. Hayashi, A. Inoue and T. Masumoto: "Rapidly solidified powder metallurgy Mg97Zn1Y2 alloys with excellent tensile yield strength above 600MPa", Mater. Trans. 42 (2001), pp. 1172-1176
6. E.Abe, Y.Kawamura, K.Hayashi and A.Inoue: ""Long-period ordered structure in a high-strenght manocrystalline Mg-1at%Zn-2at%Y alloy studied by atomic-resolution Z-contrast STEM", Acta Mater. 50 (2002), pp. 3845-3857
7. T.Itoi, T.Seimiya, Y.Kawamura and M.Hirohashi: "Long period stacking structures observed in Mg97Zn1Y2 alloy", Scr. Mater. 51 (2004), pp. 107-111
8. M.Yamasaki, T.Anan, S.Yoshimoto and Y.Kawamura: "Mechanical properties of warm-extruded Mg-Zn-Gd alloy with coherent 14H long periodic stacking ordered structure precipitate", Scr. Mater. 53 (2005), pp. 799-803
9. M.Yamasaki, M.Sasaki, M.Nishijima, K.Hiraga and Y.Kawamura: "Formation of 14H long period stacking ordered structure and profuse stacking faults in Mg-Zn-Gd alloys during isothermal aging at high temperature", Acta Mater. 55 (2007), pp. 6798-6805
10. Y.Kawamura and M.Yamasaki: " Formation and mechanical properties of Mg97Zn1RE2 alloys with long-period stacking ordered structure", Mater. Trans. 48 (2007), pp. 2986-2992
11. K.Yamada, Y.Okubo, M.Shiono, H.Watanabe, S.Kamado and Y.Kojima: "Alloy development of high toughness Mg-Gd-Y-Zn Zr alloys", Mater. Trans. 47 (2006), pp. 1066-1070
12. K.Yamada, Y.Okubo, S.Kamado and Y.Kojima: "Precipitate microstructures of high strength Mg-Gd-Y-Zn-Zr alloys", Advanced Materials Research 11-12 (2006), pp. 417-420
13. T.Honma, T.Ohkubo, S.Kamado and K.Hono: "Effect of Zn additions on the age-hardening of Mg-2.0Gd-1.2Y-0.2Zr alloys", Acta Materialia 55 (2007), pp. 4137-4150
14. Y.Gao, Q.Wang, J.Gu, Y.Zhao and D.Yin: "Comparison of microstructure in Mg-10Y-5Gd-0.5Zr and Mg-10Y-5Gd-2Zn-0.5Zr alloys by conventional casting", J of Alloys and Compounds 477 (2009), pp. 374-378